



HAL
open science

Electrophoretic deposition of $\text{Li}_4\text{Ti}_5\text{O}_{12}$ nanoparticles with a novel additive for Li-ion microbatteries

Nana Amponsah Kyeremateng, Ty Mai Dinh, David Pech

► **To cite this version:**

Nana Amponsah Kyeremateng, Ty Mai Dinh, David Pech. Electrophoretic deposition of $\text{Li}_4\text{Ti}_5\text{O}_{12}$ nanoparticles with a novel additive for Li-ion microbatteries. RSC Advances, 2015, 5 (76), pp.61502 - 61507. 10.1039/c5ra11039d . hal-01873373

HAL Id: hal-01873373

<https://laas.hal.science/hal-01873373v1>

Submitted on 13 Sep 2018

HAL is a multi-disciplinary open access archive for the deposit and dissemination of scientific research documents, whether they are published or not. The documents may come from teaching and research institutions in France or abroad, or from public or private research centers.

L'archive ouverte pluridisciplinaire **HAL**, est destinée au dépôt et à la diffusion de documents scientifiques de niveau recherche, publiés ou non, émanant des établissements d'enseignement et de recherche français ou étrangers, des laboratoires publics ou privés.

PAPER

CrossMark
click for updatesCite this: *RSC Adv.*, 2015, 5, 61502

Electrophoretic deposition of $\text{Li}_4\text{Ti}_5\text{O}_{12}$ nanoparticles with a novel additive for Li-ion microbatteries†

Nana Amponsah Kyeremateng,^{ab} Ty Mai Dinh^{ab} and David Pech^{*ab}

Electrophoretic deposition is presented as a handy and cost-effective technique to transfer nano-sized (powdered) electrode materials into thin- or thick-films for electrochemical energy storage applications. Electrophoretic deposition of $\text{Li}_4\text{Ti}_5\text{O}_{12}$ nanoparticles is studied to prepare thick films as anodes for Li-ion microbatteries with MgCl_2 additives – for the first time – as an efficient charging agent and a source of binder simultaneously. Electrochemical measurements in lithium test cells confirmed that the prepared thick-film $\text{Li}_4\text{Ti}_5\text{O}_{12}$ electrode has good discharge (lithiation) capacities and cyclability, as well as good electronic and Li^+ transport properties. Indeed, electrophoretic deposition is demonstrated to be a suitable alternative to prepare self-supported micro- or nano-structured $\text{Li}_4\text{Ti}_5\text{O}_{12}$ for Li-ion microbatteries.

Received 10th June 2015
Accepted 10th July 2015

DOI: 10.1039/c5ra11039d

www.rsc.org/advances

Introduction

In recent years, all-solid-state Li-ion microbatteries have gained exceptional significance because of the need for energy supply/storage in microelectronic devices such as medical implants, hearing aids, “smart” cards, RF-ID tags, remote sensors and energy harvesters, which are increasingly becoming inevitable in our modern society.^{1,2} Conventionally, microbatteries are two-dimensional, comprising thin-film ceramic materials as anode, electrolyte and cathode. They are fabricated by sequential layer-by-layer deposition of the cell components using physical-vapour-deposition (PVD) techniques, and have quite small dimensions ($\sim 1 \text{ cm}^3$).¹ However, the present or the future miniaturization of microelectronic devices necessitates size diminution of the microbatteries ($\leq 0.1 \text{ cm}^3$); in addition, higher energy or power densities are also required.³ These factors have underscored the need for different processing steps to be evaluated for possible micro- or nano-structuring of the electrode materials for microbatteries.^{1,2,4}

Furthermore, as a result of fabrication and application limitations, significant efforts are being made to avoid the use of metallic lithium, thus transposing the “Li-ion” or the “rocking-chair” concept to microbatteries.¹ Actually, the choice of the positive or the negative electrode material to fabricate a Li-ion microbattery is not as problematic as the choice of the processing step needed to transfer the powdered material into a

thin/thick film well-supported on the preferred current collector. Despite the fact that the physical vapour deposition (DC or RF magnetron sputtering, pulse laser deposition, *etc.*) techniques typically used for depositing electrode materials for microbatteries are quite expensive, their top-down deposition nature does not also meet the need to conformally deposit electrode materials onto high-aspect-ratio current collectors. Although CVD techniques and their derivatives can help to obtain conformal coatings of electrode materials, just like PVD, they are expensive and heating of the substrate during deposition or annealing of the obtained coating is usually needed to ensure crystallinity for optimum battery performance.^{5,6}

For some time now, solution-based processing (electrolytic deposition,^{7,8} electrophoretic deposition,^{9–11} sol-gel deposition,¹² serigraphy,¹³ ink-jet printing,¹⁴ chemical bath deposition¹⁵ *etc.*) of electrode materials has been demonstrated to be handy and cost-effective in preparing thin-film electrodes for improved electrochemical energy storage. Among the solution-based deposition techniques, electrophoretic deposition is currently gaining attention for preparing self-supported electrodes for microbatteries, especially due to the fact that the crystallinity of the starting powder is always retained in the deposited thick film.^{16–18} Electrophoretic deposition is a simple, versatile, scalable and relatively inexpensive route for preparing thick films; and it requires only an electric field and a suspension of charged particles. As the electrophoretic deposition begins from the electrode–electrolyte interface, it is envisaged to be a useful technique to conformally coat substrates of high aspect ratios with electrode materials, especially once enough wetting is achieved; this has been recently demonstrated by Mazor *et al.*¹⁶ with LiFePO_4 and a gold-coated perforated silicon substrate.

^aLAAS-CNRS (UMR 8001), 7 avenue du Colonel Roche, F-31077 Toulouse, France.
E-mail: dpech@laas.fr; Fax: +33 5 61 33 62 08; Tel: +33 5 61 33 68 37

^bUniversity of Toulouse, LAAS, F-31400 Toulouse, France

† Electronic supplementary information (ESI) available. See DOI: 10.1039/c5ra11039d

However, one setback with the electrophoretic deposition process is the difficulty in choosing the right charging agent.^{10,18–20} Apart from toxicity considerations and chemical compatibility with the electrode materials, not all charging agents impart enough charge to the particles for a very stable suspension. In this work, electrophoretic deposition of $\text{Li}_4\text{Ti}_5\text{O}_{12}$ (lithium–titanate) nanoparticles is studied to prepare thick films as anodes for Li-ion microbatteries with MgCl_2 additive – for the first time – as an efficient charging agent and a source of a binder simultaneously.

Experimental section

Elaboration of the electrodes

$\text{Li}_4\text{Ti}_5\text{O}_{12}$ nanopowder (Sigma-Aldrich, >99%) was used as received. A suspension was made with 1 g L^{-1} of $\text{Li}_4\text{Ti}_5\text{O}_{12}$, and 0.1 g L^{-1} of MgCl_2 (ACROS Organics, Pure) as the charging agent in a solvent of 95% ethanol and 5% water. Pulsed-potential electrophoretic deposition was achieved with a platinum foil counter electrode and an electric field of 32 V cm^{-1} at a duty cycle of 50% ($t_{\text{on}} = t_{\text{off}} = 3 \text{ ms}$) using Rohde–Schwarz NGSM 32/10 generator. The substrate used for the deposition consisted of Cu thin-film (400 nm) prepared by evaporation onto Si (with a 600 nm surface layer of SiO_2 – obtained by thermal oxidation).

Material characterizations

The samples, after the deposition, were dried at $120 \text{ }^\circ\text{C}$ for 2 hours. Optional X-ray-diffraction studies were carried-out at room temperature with a step-time of 10 s and step-size of 0.02° using a D8 Advance Bruker (Karlsruhe, Germany) diffractometer with Cu $K\alpha$ radiation (1.5406 \AA). Energy-dispersive X-ray spectroscopy (EDS) analysis and scanning electron microscopy (SEM) were performed using a Hitachi S-4800 field-emission electron microscope. Thickness measurements were carried out with Tencor profilometer. The mass of the deposited $\text{Li}_4\text{Ti}_5\text{O}_{12}$ was obtained by means of a weight difference before and after deposition, using Sartorius precision balance.

Electrochemical measurements

For the electrochemical measurements, two-electrode EL-Cells were assembled in a glove-box filled with purified argon in which moisture and oxygen contents were less than 2 ppm. The galvanostatic experiments were then carried out with the prepared Li/LiPF_6 (EC:DEC)/ $\text{Li}_4\text{Ti}_5\text{O}_{12}$ cells using VMP3 potentiostat/galvanostat. The electrolyte supplied by Solvionic was embedded in a Whatman glass microfiber – which acts as a separator. Additionally, cyclic voltammetry was carried out with the VMP3 potentiostat/galvanostat in the $1 \leq U \text{ (V)} \leq 3$ voltage range at a scan rate of 0.1 mV s^{-1} . Electrochemical impedance spectroscopy was carried out with a VMP3 potentiostat/galvanostat equipped with a frequency response analyzer. The frequency range was 100 KHz to 100 mHz with 10 mV AC voltage amplitude. The fitting of the experimental data was achieved with the EC-lab software.

Results and discussions

Morphology and composition

$\text{Li}_4\text{Ti}_5\text{O}_{12}$ has been well studied and is presently used as an anode material in commercial Li-ion batteries;^{1,21} as a consequence, interest has arisen to adopt it for Li-ion microbatteries. Electrophoretic deposition of $\text{Li}_4\text{Ti}_5\text{O}_{12}$ had been reported by Munakata *et al.*²² – for Li-ion microbatteries – with iodine as the charging agent, Ketjen Black as the conductive medium linking the deposited particles, and polyethylene oxide as the binder. This combination of additives is sometimes not optimum for a stable suspension and hence, surfactants might be required to improve the stability of the suspension.¹⁶ In 2010, Pech *et al.*²³ reported that MgCl_2 can be used as a charging agent for the electrophoretic deposition of carbon films for micro-supercapacitor applications. In their work, the Mg^{2+} cations were well-adsorbed on the carbon particles for effective electrophoretic deposition; also hydroxyl ions accumulated near the working electrode reacted with Mg^{2+} cations to form $\text{Mg}(\text{OH})_2$ which acts as an inorganic binder for the deposited particles.

As yet, such approach of electrophoretic deposition – without a surfactant nor a binder – had not been tested with electrode materials for lithium storage. Indeed, a stable suspension (~ 4 days) was obtained with the $\text{Li}_4\text{Ti}_5\text{O}_{12}$ nanoparticles (average particle size of $\sim 50 \text{ nm}$) and the MgCl_2 additive: zeta potential (ζ) of +26 mV and size-in-solution of $\sim 600 \text{ nm}$ were measured with *Zetasizer nanoseries* from Malvern Instruments. Pulse-potential electrophoretic deposition was adopted for this study, because it has already been demonstrated to give better deposits than constant-potential electrophoretic deposition.¹⁹ According to the SEM micrographs ((a) surface; (b) cross-section) shown in Fig. 1, the thickness obtained after 5 min of deposition is $\sim 3.3 \text{ }\mu\text{m}$. Indeed, the electrophoretic deposition proceeds, for the most part, with the very small $\text{Li}_4\text{Ti}_5\text{O}_{12}$ nanoparticles ($\sim 50 \text{ nm}$) stable in the suspension. It can also be noticed – in Fig. 1(a) – that some cracks as well as surface porosity exist in the deposited $\text{Li}_4\text{Ti}_5\text{O}_{12}$ layers. So far as EPD is concerned, it has been well established that such discontinuities can be overcome if the particles in the suspension have very high surface charge ($|\zeta| \geq 40 \text{ mV}$).^{10,18} On the other hand, such discontinuities can be advantageous for lithium storage applications because of the concomitant higher surface area.

Interestingly, it can be noticed – in Fig. 1(b) – that the deposited $\text{Li}_4\text{Ti}_5\text{O}_{12}$ layer is still intact even after cleaving the substrate for SEM observation of the cross-section; this is an indication of the good binding effect of the formed $\text{Mg}(\text{OH})_2$. In fact, energy dispersive X-ray analysis (Fig. S1, ESI[†]) confirmed the presence of Mg, Ti and O in the deposited layer, in addition to Cu from the current collector and Si from the substrate. A mapping was done (Fig. S1, ESI[†]) and it showed a uniform distribution of Mg on all the deposited $\text{Li}_4\text{Ti}_5\text{O}_{12}$ particles. Actually, as anticipated, the thickness of the deposited $\text{Li}_4\text{Ti}_5\text{O}_{12}$ layer and the corresponding mass increased with increasing deposition time as showcased in Fig. 2. Moreover, according to the X-ray diffraction pattern presented in Fig. S2 (ESI[†]), the

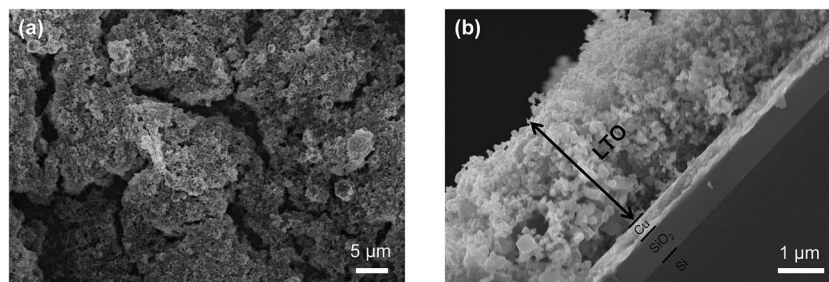


Fig. 1 SEM micrograph ((a) surface; (b) cross-section) of the $\text{Li}_4\text{Ti}_5\text{O}_{12}$ deposits obtained at $E = 32 \text{ V cm}^{-1}$ in a 1 g L^{-1} $\text{Li}_4\text{Ti}_5\text{O}_{12}$ suspension (0.1 g L^{-1} of MgCl_2 , 95% ethanol – 5% water) during 5 min.

crystallinity of the $\text{Li}_4\text{Ti}_5\text{O}_{12}$ powder was conserved in the deposited layers. The diffractogram also indicated the presence of an infinitesimal proportion of rutile TiO_2 in the original $\text{Li}_4\text{Ti}_5\text{O}_{12}$ powder. It can also be noticed that, apart from the diffraction peaks of Cu from the current collector and Si from the substrate, no additional peaks were identified for $\text{Mg}(\text{OH})_2$ in the deposited layers, indicating that the formed $\text{Mg}(\text{OH})_2$ is amorphous with this preparation procedure.

It has been well studied and well documented in literature^{24–26} that, during EPD with such deposition baths, OH^- produced by the reduction of water at the negative electrode reacts with the Mg^{2+} cations adsorbed on the particle surface, forming $\text{Mg}(\text{OH})_2$ precipitates around the deposited particles. In fact, the binding effect of the $\text{Mg}(\text{OH})_2$ precipitates was also confirmed with adhesion tests. It has been well demonstrated¹ with FTIR spectroscopy that, when the water content is far less than 5 vol%, the precipitate even consists mostly of $\text{Mg}(\text{C}_3\text{H}_7\text{O})_2$ alkoxide, but $\text{Mg}(\text{OH})_2$ predominates with at least 5 vol% water. As evidenced with our XRD experiments, and in accordance with literature,²⁶ the precipitated $\text{Mg}(\text{OH})_2$ is not crystalline.

Electrochemical properties

Furthermore, electrochemical measurements were carried out in a half-cell configuration to evaluate the performance of the deposited $\text{Li}_4\text{Ti}_5\text{O}_{12}$ as an anode material for Li-ion micro-batteries. All the samples used for the electrochemical studies

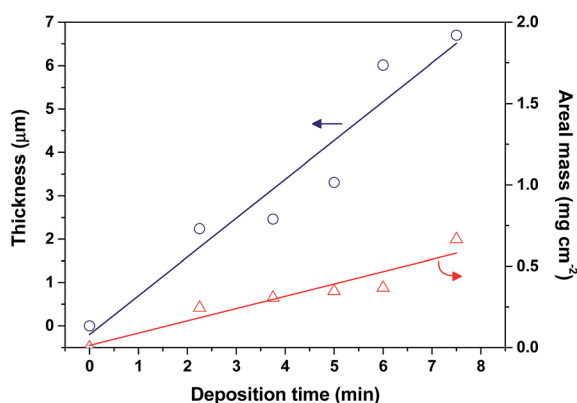


Fig. 2 Evolution of the thickness and the mass with deposition time for the $\text{Li}_4\text{Ti}_5\text{O}_{12}$ deposits prepared at $E = 32 \text{ V cm}^{-1}$ in a 1 g L^{-1} $\text{Li}_4\text{Ti}_5\text{O}_{12}$ suspension (0.1 g L^{-1} of MgCl_2 , 95% ethanol – 5% water).

were prepared under the same conditions, and they are all expected to be *ca.* $3.3 \mu\text{m}$ thick. The galvanostatic cycle life performance of the deposited $\text{Li}_4\text{Ti}_5\text{O}_{12}$ is presented in Fig. 3(a and b). The resulting specific discharge (lithiation) capacities *versus* cycle number decrease slightly from 0.5C to 2C (see Fig. 3(a)), which is an indication of good rate performance. It is worth emphasizing that the lithiation capacities evolve around the theoretical value of 175 mA h g^{-1} as typically reported⁶ for $\text{Li}_4\text{Ti}_5\text{O}_{12}$ – with negligible capacity fading. After extended cycling at 2C, Coulombic efficiency of 99.5% was obtained with 65 cycles (see Fig. 3(b)). As there is no SEI formation for $\text{Li}_4\text{Ti}_5\text{O}_{12}$ electrodes, the very high lithiation capacities observed in the first few cycles can be substantiated by side reactions with solvent traces in the deposited $\text{Li}_4\text{Ti}_5\text{O}_{12}$ layers. Measures such as protracted drying at temperatures above $120 \text{ }^\circ\text{C}$ are currently underway to help eliminate the solvent traces and the concomitant side reactions with lithium. Additionally, as shown in Fig. 4(a), the prepared $\text{Li}_4\text{Ti}_5\text{O}_{12}$ electrodes exhibit the lithium insertion/extraction plateaus characteristic of $\text{Li}_4\text{Ti}_5\text{O}_{12}$ in the usual $1 \leq U \text{ (V)} \leq 3$ voltage window.

The proportion of $\text{Mg}(\text{OH})_2$ in the deposited $\text{Li}_4\text{Ti}_5\text{O}_{12}$ electrodes is about 10 wt%, and its presence does not seem to have any adverse effect on the electrochemical behaviour of the deposited $\text{Li}_4\text{Ti}_5\text{O}_{12}$. Also, the cyclic voltammogram (see Fig. 4(b)) recorded at 0.1 mV s^{-1} for the $\text{Li}_4\text{Ti}_5\text{O}_{12}$ electrode agreed with what has already been reported for this material,²⁷ and did not indicate the presence of additional peaks for any side reactions. As a matter of fact, an electrode of pure $\text{Mg}(\text{OH})_2$ was prepared by EPD under the same conditions, but it showed negligible lithium storage when tested *vs.* lithium in the same potential window. Intriguingly, without carbon coating of the $\text{Li}_4\text{Ti}_5\text{O}_{12}$ particles nor carbon black additive, the $\text{Mg}(\text{OH})_2$ tends to have enough electronic conductivity to link the deposited $\text{Li}_4\text{Ti}_5\text{O}_{12}$ nanoparticles for good rate performance, considering that pure $\text{Li}_4\text{Ti}_5\text{O}_{12}$ has not a very good electronic conductivity.²⁸ Certainly, $\text{Mg}(\text{OH})_2$ is not insulating; it has been reported²⁹ that $\text{Mg}(\text{OH})_2$ films can have electronic conductivity as moderate as 10^{-4} to $10^{-5} \text{ S cm}^{-1}$. Also, it can be noticed in Fig. 4(a) that, after the typical flat discharge/charge plateaus, the voltage profiles up to the upper or lower cut-off potentials are not as vertical as usually obtained for $\text{Li}_4\text{Ti}_5\text{O}_{12}$ electrodes. The effect is also marginally evident from the cyclic voltammogram curves presented in Fig. 4(b) at *ca.* 1.4 V and $2.25 \text{ V vs. Li}^+/\text{Li}$.

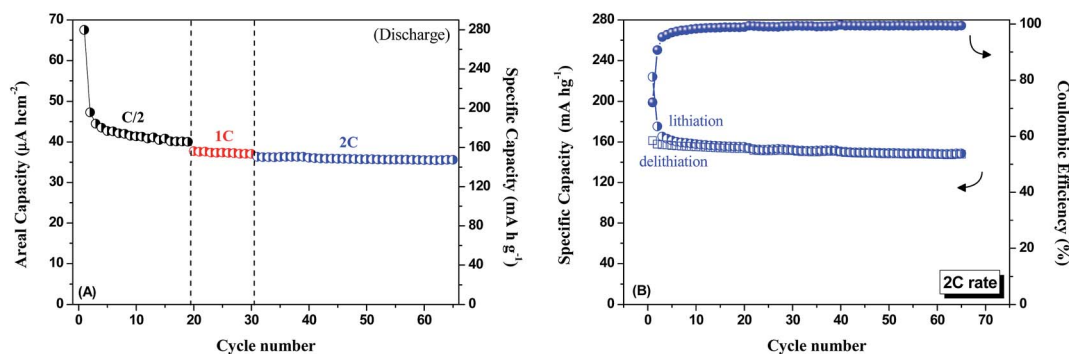


Fig. 3 (a) Specific capacity vs. cycle number and (b) Coulombic efficiency for the electrophoretically prepared $\text{Li}_4\text{Ti}_5\text{O}_{12}$ electrodes.

This behaviour is truly enigmatic and although efforts of elucidation are underway, additional lithium reaction with the infinitesimal rutile TiO_2 , and possible interfacial lithium storage due to the morphology of the electrodes are worth considering.

Furthermore, in an attempt to carry out post-mortem SEM for one cycled electrode, the El-cell was opened and the electrode washed in the glove-box; the electrode was washed gently by immersing in isopropanol and shaking for some seconds; afterwards, the electrode was dried under vacuum at 60°C for 1 h. Truly, by visual inspection, no particles had peeled off before the gentle washing. However, it became visually obvious that some particles peeled off during the washing. Similar peel-offs (macroscopic cavities) were observed for a pristine electrode subjected to the same procedure. It can thus be asserted that, SEM will not show the peel-off solely due to electrochemical cycling as there is peel-off from the washing. All the same, it is believed that the deposit remains intact before and after the electrochemical tests according to the good capacity retention shown in Fig. 3, but the adhesion may have to be improved in order to withstand such rare post-mortem handling.

For proper benchmarking of the electrophoretically deposited carbon-free $\text{Li}_4\text{Ti}_5\text{O}_{12}$ electrodes, electrochemical

impedance spectroscopy (EIS) and chronoamperometry experiments were carried out to ascertain the charge transfer resistance and the Li^+ ion diffusion coefficient. The impedance measurement was carried out after the first discharge-charge cycle, and the obtained spectrum is presented in Fig. 5(a); the solid line superimposing the data points corresponds to the calculated values of the impedance obtained by fitting with the equivalent-circuit model shown in the inset of Fig. 5(a). The equivalent circuit consists of the electrolyte resistance R_e , the charge-transfer resistance R_{ct} , the Warburg resistance Z_w , and the constant phase element (CPE). In effect, the charge transfer resistance was estimated to be $103 \Omega \text{ cm}^2$, which is far better than what was reported for other $\text{Li}_4\text{Ti}_5\text{O}_{12}$ thin film electrodes.^{6,30}

In addition, we carried out potentiostatic experiments for which the current-transient profiles before the onset of a limiting current can be described by the Cottrell equation:^{31,32}

$$j = nFD_o^{1/2}C_o\pi^{-1/2}t^{-1/2} \quad (1)$$

where (j) is the current density and (t) the time. The potentiostatic experiments consisted of applying a potential step (from 3.0 to 1.2 V vs. Li^+/Li) to cells of Li/LiPF_6 (EC:DEC)/ $\text{Li}_4\text{Ti}_5\text{O}_{12}$

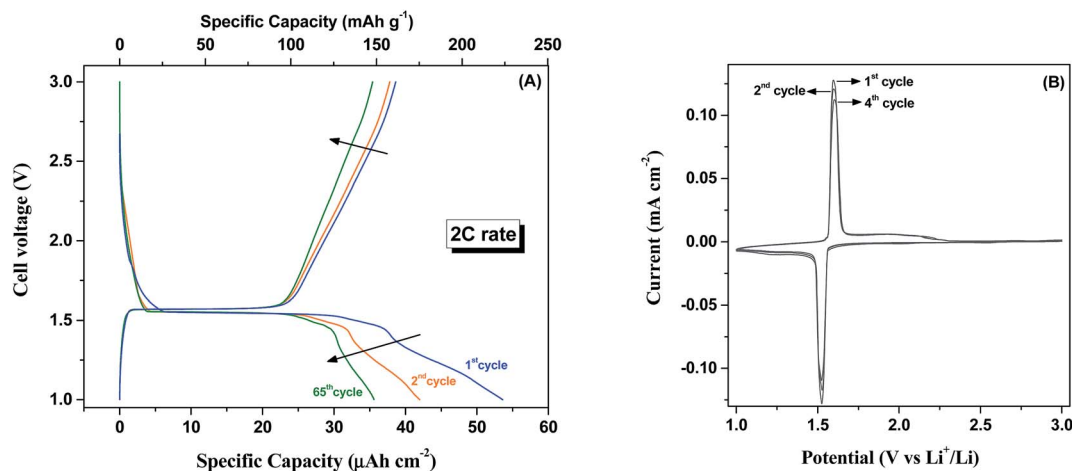


Fig. 4 (a) Galvanostatic lithium insertion/extraction profiles and (b) cyclic voltammogram recorded at 0.1 mV s^{-1} for the prepared $\text{Li}_4\text{Ti}_5\text{O}_{12}$ electrodes.

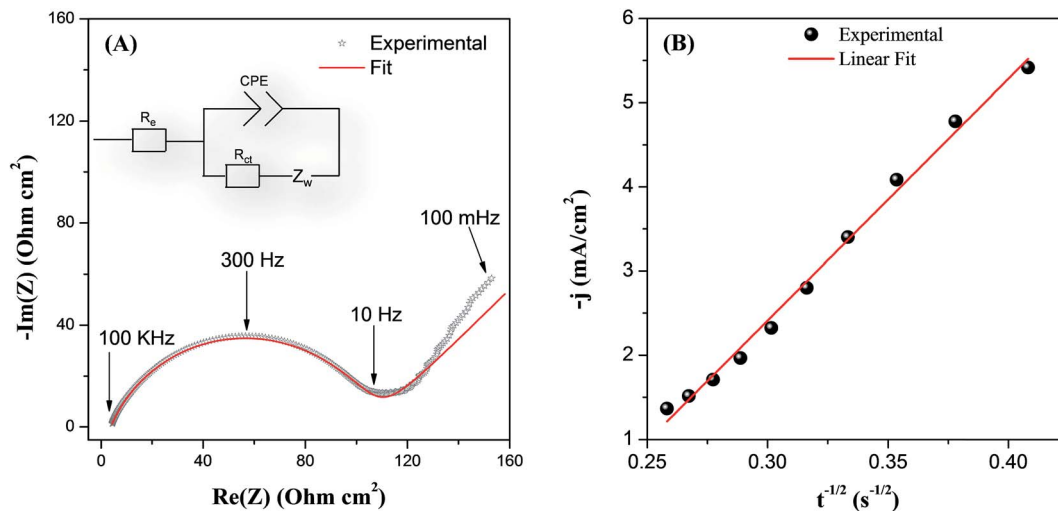


Fig. 5 (a) Nyquist plots and (b) Cottrell plot obtained for the electrophoretically deposited $\text{Li}_4\text{Ti}_5\text{O}_{12}$ electrodes.

during 30 s. Knowing that 3 Li^+ ions are inserted per mol of $\text{Li}_4\text{Ti}_5\text{O}_{12}$, the concentration of Li^+ (C_0) was calculated to be $24.4 \times 10^{-3} \text{ mol cm}^{-3}$ using 3.7 g cm^{-3} density of $\text{Li}_4\text{Ti}_5\text{O}_{12}$. Hence, the diffusion coefficient (D_0) was estimated from the slope of the fit to the Cottrell plot (Fig. 5(b)) to be $5.2 \times 10^{-11} \text{ cm}^2 \text{ s}^{-1}$ – which is an indication of good lithium transport properties in the electrophoretically deposited $\text{Li}_4\text{Ti}_5\text{O}_{12}$ thick film. Indeed, this value of diffusion coefficient agrees with what has been previously reported with GITT and Impedance techniques for $\text{Li}_4\text{Ti}_5\text{O}_{12}$ thin films.^{30,33}

Although various deposition procedures have been reported for preparing thin-film $\text{Li}_4\text{Ti}_5\text{O}_{12}$ electrodes,^{30,33,34} electrophoretic deposition is esteemed to be much simple and cost-effective and can be a suitable alternative to prepare self-supported micro- or nano-structured $\text{Li}_4\text{Ti}_5\text{O}_{12}$ for Li-ion microbatteries.

Conclusions

Electrophoretic deposition of $\text{Li}_4\text{Ti}_5\text{O}_{12}$ nanoparticles is studied to prepare thick films as anodes for Li-ion microbatteries with MgCl_2 additive – for the first time – as an efficient charging agent and a source of a binder simultaneously. X-ray diffraction studies confirmed that the crystallinity of the $\text{Li}_4\text{Ti}_5\text{O}_{12}$ powder was conserved in the deposited layer. Electrochemical measurements in lithium test cells confirmed that the prepared thick-film $\text{Li}_4\text{Ti}_5\text{O}_{12}$ electrode has good discharge (lithiation) capacities and cyclability. Electrochemical impedance spectroscopy and chronoamperometry experiments were used to ascertain the charge transfer resistance ($103 \Omega \text{ cm}^2$) and the Li^+ ion diffusion coefficient ($5.2 \times 10^{-11} \text{ cm}^2 \text{ s}^{-1}$), confirming good electronic and lithium transport properties in the electrophoretically deposited $\text{Li}_4\text{Ti}_5\text{O}_{12}$ thick films. Measures are being taken to eliminate the solvent traces and improve the initial Coulombic efficiencies of the first few cycles; and also elucidate the sloping profiles observed after the discharge/charge plateaus. Indeed, electrophoretic deposition is demonstrated

to be a suitable alternative to prepare self-supported micro- or nano-structured $\text{Li}_4\text{Ti}_5\text{O}_{12}$ for 3D Li-ion microbatteries, especially with micro- or nano-structured current collectors.

Acknowledgements

This work was partly supported by the French RENATECH network and financially supported by the FP7 MATFLEXEND Project (# 604093). We also express much appreciation to Xavier Dollat of LAAS-CNRS mechanical workshop, for the design and the fabrication of the deposition cell.

References

- 1 N. A. Kyeremateng, *ChemElectroChem*, 2014, **1**, 1442–1466.
- 2 J. F. M. Oudenhoven, L. Baggetto and P. H. L. Notten, *Adv. Energy Mater.*, 2011, **1**, 10–33.
- 3 B. Warneke, M. Last, B. Liebowitz and K. S. J. Pister, *Computer*, 2001, **34**, 44–51.
- 4 J. Xu, X. Wang, X. Wang, D. Chen, X. Chen, D. Li and G. Shen, *ChemElectroChem*, 2014, **1**, 975–1002.
- 5 H. C. M. Knoops, M. E. Donders, M. C. M. van de Sanden, P. H. L. Notten and W. M. M. Kessels, *J. Vac. Sci. Technol., A*, 2012, **30**, 010801.
- 6 J. Deng, Z. Lu, I. Belharouak, K. Amine and C. Y. Chung, *J. Power Sources*, 2009, **193**, 816–821.
- 7 N. A. Kyeremateng, C. Lebouin, P. Knauth and T. Djenizian, *Electrochim. Acta*, 2013, **88**, 814–820.
- 8 T. M. Dinh, A. Achour, S. Vizireanu, G. Dinescu, L. Nistor, K. Armstrong, D. Guay and D. Pech, *Nano Energy*, 2014, **10**, 288–294.
- 9 J. H. Jang, K. Machida, Y. Kim and K. Naoi, *Electrochim. Acta*, 2006, **52**, 1733–1741.
- 10 I. Corni, M. P. Ryan and A. R. Boccaccini, *J. Eur. Ceram. Soc.*, 2008, **28**, 1353–1367.
- 11 T. M. Dinh, K. Armstrong, D. Guay and D. Pech, *J. Mater. Chem. A*, 2014, **2**, 7170–7174.

- 12 M. Beidaghi and Y. Gogotsi, *Energy Environ. Sci.*, 2014, **7**, 867–884.
- 13 H. Durou, D. Pech, D. Colin, P. Simon, P.-L. Taberna and M. Brunet, *Microsyst. Technol.*, 2012, **18**, 467–473.
- 14 D. Pech, M. Brunet, P.-L. Taberna, P. Simon, N. Fabre, F. Mesnilgrente, V. Conédéra and H. Durou, *J. Power Sources*, 2010, **195**, 1266–1269.
- 15 X. Xia, Y. Zhang, D. Chao, C. Guan, Y. Zhang, L. Li, X. Ge, I. M. Bacho, J. Tu and H. J. Fan, *Nanoscale*, 2014, **6**, 5008–5048.
- 16 H. Mazon, D. Golodnitsky, L. Burstein, A. Gladkikh and E. Peled, *J. Power Sources*, 2012, **198**, 264–272.
- 17 A. Caballero, L. Hernan, M. Melero, J. Morales, R. Moreno and B. Ferrari, *J. Power Sources*, 2006, **158**, 583–590.
- 18 L. Besra and M. Liu, *Prog. Mater. Sci.*, 2007, **52**, 1–61.
- 19 M. Ammam, *RSC Adv.*, 2012, **2**, 7633–7646.
- 20 M. S. Ata, Y. Liu and I. Zhitomirsky, *RSC Adv.*, 2014, **4**, 22716–22732.
- 21 G.-N. Zhu, Y.-G. Wang and Y.-Y. Xia, *Energy Environ. Sci.*, 2012, **5**, 6652–6667.
- 22 H. Munakata, T. Sugiura and K. Kanamura, *Funct. Mater. Lett.*, 2009, **2**, 9–12.
- 23 D. Pech, M. Brunet, H. Durou, P. Huang, V. Mochalin, Y. Gogotsi, P.-L. Taberna and P. Simon, *Nat. Nanotechnol.*, 2010, **5**, 651–654.
- 24 B. E. Russ and J. B. Talbot, *J. Electrochem. Soc.*, 1998, **145**, 1245–1252.
- 25 C. Du and N. Pan, *J. Power Sources*, 2006, **160**, 1487–1494.
- 26 E. de Beer, J. Duval and E. A. Meulenkamp, *J. Colloid Interface Sci.*, 2000, **222**, 117–124.
- 27 C. Zhang, Y. Zhang, J. Wang, D. Wang, D. He and Y. Xia, *J. Power Sources*, 2013, **236**, 118–125.
- 28 C. Lin, B. Ding, Y. Xin, F. Cheng, M. O. Lai, L. Lu and H. Zhou, *J. Power Sources*, 2014, **248**, 1034–1041.
- 29 J. Gasc, F. Brunet, N. Bagdassarov and V. Morales-Florez, *Phys. Chem. Miner.*, 2011, **38**, 543–556.
- 30 J. Deng, Z. Lu, C. Y. Chung, X. Han, Z. Wang and H. Zhou, *Appl. Surf. Sci.*, 2014, **314**, 936–941.
- 31 L. Kavan, M. Grätzel, S. E. Gilbert, C. Klemenz and H. J. Scheel, *J. Am. Chem. Soc.*, 1996, **118**, 6716–6723.
- 32 N. A. Kyeremateng, F. Vacandio, M. T. Sougrati, H. Martinez, J. C. Jumas, P. Knauth and T. Djenizian, *J. Power Sources*, 2013, **224**, 269–277.
- 33 F. Wunde, F. Berkemeier and G. Schmitz, *J. Power Sources*, 2012, **215**, 109–115.
- 34 J. Mosa, J. F. Velez, J. J. Reinoso, M. Aparicio, A. Yamaguchi, K. Tadanaga and M. Tatsumisago, *J. Power Sources*, 2013, **244**, 482–487.